

# Quantum Projector Method on Curved Manifolds

V. Melik-Alaverdian<sup>a</sup>, G. Ortiz<sup>b</sup>, and N. E. Bonesteel<sup>c</sup>

<sup>a</sup> *Department of Physics, University of Rhode Island, Kingston, RI 02881*

<sup>b</sup> *Theoretical Division, Los Alamos National Laboratory, P.O. Box 1663, Los Alamos, NM 87545*

<sup>c</sup> *National High Magnetic Field Laboratory and Department of Physics, Florida State University, Tallahassee, FL 32306-4005*

(October 29, 2018)

## Abstract

A generalized stochastic method for projecting out the ground state of the quantum many-body Schrödinger equation on curved manifolds is introduced. This random-walk method is of wide applicability to any second order differential equation (first order in time), in any spatial dimension. The technique reduces to determining the proper “quantum corrections” for the Euclidean short-time propagator that is used to build up their path-integral Monte Carlo solutions. For particles with Fermi statistics the “Fixed-Phase” constraint (which amounts to fixing the phase of the many-body state) allows one to obtain stable, albeit approximate, solutions with a variational property. We illustrate the method by applying it to the problem of an electron moving on the surface of a sphere in the presence of a Dirac magnetic monopole.

Pacs Numbers: 2.70.Lq, 5.30.Fk, 71.10.Pm, 73.20.Dx

## I. INTRODUCTION

The importance and difficulty of solving models of interacting quantum particles is hard to overstate. It is well known that the correlated motion of those particles gives rise to a wide variety of physical phenomena at different length and time scales, spanning disciplines like chemistry, condensed matter, nuclear, and high energy physics. Novel complex structures can emerge as a consequence of the competing multiple-length scales in the problem. Nonetheless, only a reduced set of interacting problems admits exact closed form solutions [1] and the use of numerical techniques becomes essential if one is looking for accurate solutions not subjected to uncontrolled approximations. Among those techniques, the statistical methods [2] offer the potential to study systems with large number of degrees of freedom, reducing the computational complexity from exponential to polynomial growth. This scaling behavior is particularly relevant when one recognizes that most of the interesting phenomena in many-body physics occurs in the thermodynamic limit [3]. Unfortunately, for fermions (i.e. quantum particles obeying Fermi statistics) the sign problem plagues all useful stochastic algorithms and causes the variance of computed results to increase exponentially with increasing number of fermions [4].

On the other hand, the growing interest in physical systems whose state functions are defined on a general metric space makes the quantum mechanics of interacting particles in curved manifolds no longer a mere intellectual exercise, but one with very practical consequences. Perhaps the most well-known examples can be found in cosmology (e.g., matter in strong gravitational fields, atomic spectroscopy as probe of space-time curvature [5]), but the subject is certainly not exclusive to this field. In condensed matter a very elementary case is provided by a deformed crystal. Less well-known ones are mesoscopic graphitic microtubules and fullerenes. All these physical systems are ubiquitous in nature and the crucial role the curvature of the manifold plays has been confirmed by experimental observations (e.g. spectrum of collective excitations [6]). Therefore, the development of stable quantum methods with polynomial complexity in Riemannian manifolds represents a real challenge for many-body theorists.

The present manuscript deals with the (non-relativistic) many-particle Schrödinger equation in a general metric space and its solution using stochastic techniques. In particular, we will show how to construct approximate solutions (wave functions) for systems with broken time-reversal symmetry (e.g. electrons in the presence of external electromagnetic sources) avoiding the infamous “phase problem” [7]. The main difficulty is to define a probability measure (semi-positive definite) which allows one to get the complex-valued state with no asymptotic signal-to-noise ratio decay in Euclidean time. This translates into a problem of geometric complexity, which is solved approximately using constraints in the manifold where the wave function has its support. In this way, we get stable but approximate solutions which can be systematically improved.

Among the large variety of problems one can attack, we decided to choose the general problem of fermions in the presence of external gauge fields to illustrate the main ideas. The effects of an external magnetic field on a system of electrons can be profound [8]. The field couples to the electron’s charge and spin, modifying its spatial motion and lifting its spin degeneracies. The field can also create spatial anisotropy, effectively reducing the dimensionality of the system from three to two. The combination of the reduced dimension

and the field itself is known to have novel consequences. For example, in a system of non-interacting electrons hopping on a square lattice, the field transforms the energy spectrum from the simplicity of trigonometric functions to the complexity of a field-dependent self-similar structure (Hofstadter's butterfly) whose depth mathematicians are still fathoming [9]. The combination of the reduced dimensionality, strong particle interactions and the field itself is known to have novel consequences, like the formation of isotropic fractional quantum Hall fluids [10], which are incompressible states of the two-dimensional homogeneous Coulomb gas.

The projector (zero temperature) method we will introduce uses random-walks to solve a general multidimensional partial differential equation second order in space coordinates and first order in time. Whenever mention is made of a random-walk we mean a Markov chain that is defined as a sequence  $\mathcal{R}_1, \mathcal{R}_2, \dots, \mathcal{R}_K$  of  $K$  random variables that take values in configuration space, i.e. the space of particle positions. As usual, what characterizes a random-walk is its initial probability distribution and a conditional probability that dictates the transition from  $\mathcal{R}_i$  to  $\mathcal{R}_{i+1}$ . This transition probability is non-unique and discretization dependent [11]. Among all the possible choices we will require a prepoint discretization of the transition probability (short-time propagator) because we will use Monte Carlo methods to generate the walkers.

The paper is organized as follows. In Section II we present the formulation of the general problem of fermions in curved manifolds. In particular, for illustration purposes and to fix notation, we develop the formalism for spin- $\frac{1}{2}$  particles in the presence of an external electromagnetic potential. Then, we show how to project out the lowest energy state of a given symmetry in a manifold with curvature, and discuss the resulting Fokker-Planck equations for various distribution functions. Once the problem is precisely defined we develop, in Section III, path-integral solutions to those multidimensional differential equations, and give an interpretation of the emergent "quantum corrections" in the Euclidean action. The path-integral solutions are evaluated using Monte Carlo techniques in Section IV. There, we provide a stable step by step practical algorithm which emphasizes the subtle changes (with respect to the standard Diffusion Monte Carlo (DMC) technique) due to the metric of the manifold. In Section V we apply such computational implementation to the problem of an electron moving on the surface of a sphere in the presence of a Dirac monopole. Finally, Section VI summarizes the main findings and discusses the relevance of the stochastic method as applied to the physics of quantum Hall fluids.

## II. FERMIONS ON RIEMANNIAN MANIFOLDS

*Notation.* Consider a differentiable manifold  $\mathcal{M}$  of dimension  $d$  (e.g., for the two-sphere  $S^2$ ,  $d=2$ ) with coordinates  $\mathbf{r}_i = (x_i^1, \dots, x_i^d)$  defined on it. If  $\mathcal{M}$  is a Riemannian manifold, then it is a metric space, with metric tensor  $g^{\mu\nu}(\mathbf{r}_i) = g^{\mu\nu}(i)$ , such that the distance  $ds$  between two points in  $\mathcal{M}$  is  $ds^2 = g_{\mu\nu}(i) dx_i^\mu dx_i^\nu$  in the usual way [12]. The metric tensor is positive definite and symmetric  $g^{\mu\nu} = g^{\nu\mu}$  (as we will see, this condition is important to define a probability density distribution), and is a function of the coordinates  $\mathbf{r}_i$  with the property  $g_{\mu\gamma} g^{\gamma\nu} = \delta_\mu^\nu$ . Let us consider the coordinate transformation  $h$ :  $x_i^\mu = h^\mu(x_i'^1, \dots, x_i'^d)$ . Then, a generic second order contravariant ( $T^{\mu\nu}$ ) and covariant tensor ( $T_{\mu\nu}$ ) transform as

$$T^{\mu\nu} = \frac{\partial x_i^\mu}{\partial x_i'^\alpha} \frac{\partial x_i^\nu}{\partial x_i'^\beta} T'^{\alpha\beta} \quad , \quad T_{\mu\nu} = \frac{\partial x_i'^\alpha}{\partial x_i^\mu} \frac{\partial x_i'^\beta}{\partial x_i^\nu} T'_{\alpha\beta} \quad , \quad (1)$$

respectively. Throughout the paper Einstein's summation convention for repeated indices is assumed ( $\mu, \nu = 1, \dots, d$ ).

*Formulation of the problem.* In this article we will be concerned with finite interacting fermion systems in the presence of an external electromagnetic potential  $a_\mu(\mathbf{r}_i) = a_\mu(i) = (\mathbf{A}(i), \phi(i) = 0)$  ( $\mathbf{B} = \nabla \wedge \mathbf{A}$  represents a uniform field,  $\mathbf{A}$  and  $\phi$  are the vector and scalar potentials, respectively) whose Hamiltonian for motion on the manifold, in the coordinate representation, is given by

$$\widehat{\mathbb{H}} = \widehat{\mathbb{H}}_0 + \widehat{V}(\{\mathbf{r}_i\}, \{s_i\}) \quad (2)$$

with

$$\widehat{\mathbb{H}}_0 = -D\Delta + i\frac{e\hbar}{2m^*c} \sum_{i=1}^N \left[ 2a^\mu(i)\partial_\mu + g^{-1/2}(i)\partial_\mu \left( g^{1/2}(i)a^\mu(i) \right) \right] + \frac{e^2}{2m^*c^2} \sum_{i=1}^N a^\mu(i)a_\mu(i) \quad , \quad (3)$$

$\partial_\mu = \partial/\partial x_i^\mu$ , and  $\Delta = \sum_{i=1}^N \Delta(i)$ , where

$$\Delta = g^{-1/2}\partial_\mu \left( g^{\mu\nu} g^{1/2}\partial_\nu \right) \quad (4)$$

is the covariant Laplace-Beltrami operator and  $\widehat{V}$  is a potential energy operator. Notice that we use the conventional notation where the transformation between different forms of a given tensor is achieved by using the metric tensor (e.g.,  $a^\mu = g^{\mu\nu}a_\nu$ ,  $a_\mu = g_{\mu\nu}a^\nu$ ), and  $g^{1/2} = \sqrt{\det g_{\mu\nu}}$ . This Hamiltonian characterizes the dynamics of  $N$  non-relativistic indistinguishable particles of mass  $m^*$ , charge  $e$  and spin  $s_i = \frac{1}{2}$  in a curved space with metric tensor  $g^{\mu\nu}$ , and  $D = \hbar^2/2m^*$ . We have assumed that the quantum Hamiltonian  $\widehat{\mathbb{H}}$  in curved space has the same form as in flat space (this amounts to a particular operator ordering prescription.)

Given the previous ordering, one can rewrite the Hamiltonian above in terms of the generalized (hermitian) canonical momentum  $\mathbf{p}_\mu = -i\hbar(\partial_\mu + \frac{1}{2}\partial_\mu(\ln g^{1/2}))$

$$\widehat{\mathbb{H}} = \frac{1}{2m^*} \sum_{i=1}^N g^{-1/4}(i) \Pi_\mu g^{1/2}(i) g^{\mu\nu}(i) \Pi_\nu g^{-1/4}(i) + \widehat{V}(\{\mathbf{r}_i\}, \{s_i\}) \quad , \quad (5)$$

where the kinetic momentum  $\Pi_\mu = \mathbf{p}_\mu - \frac{e}{c}a_\mu$ . The first term in Eq. 5 represents the kinetic energy of the system and is the non-relativistic approximation to the Dirac operator.  $\widehat{V}$  includes the sum of one and two-body local interaction terms (and background potential in the case of a charge neutral system) and Zeeman contribution. The potentials are assumed to be finite almost everywhere and can only be singular at coincident points ( $\mathbf{r}_i = \mathbf{r}_j, \forall i \neq j$ )

We are interested in the stationary solutions of the resulting multidimensional Schrödinger equation

$$i\hbar \partial_t |\Psi\rangle = \widehat{\mathbb{H}} |\Psi\rangle \quad , \quad (6)$$

and will restrict ourselves to Hamiltonians  $\widehat{\mathbb{H}}$  which are time-translation invariant. In the usual space-spin formalism the  $N$ -fermion states characterizing the system,  $\langle X|\Psi\rangle = \Psi(X)$ ,

and all its first derivatives belong to the Hilbert space of antisymmetric (with respect to identical particle  $(\mathbf{r}_i, s_i)$ -exchanges) square-integrable functions  $\mathcal{H}_N = \mathcal{L}^2(\mathcal{M}^N) \otimes \mathbb{C}^{2N}$ , defined as

$$\mathcal{H}_N = \left\{ \Psi \mid \hat{P}_{ij}\Psi = -\Psi, \text{ and } \|\Psi\| = \sqrt{\langle \Psi | \Psi \rangle} < \infty \right\}, \quad (7)$$

where  $X = (\mathcal{R}, \Sigma)$  ( $\mathcal{R} = (\mathbf{r}_1, \dots, \mathbf{r}_N)$  and  $\Sigma = (\sigma_1, \dots, \sigma_N)$  are discrete spin variables) and  $\hat{P}_{ij}$  represents the permutation of the pairs  $(\mathbf{r}_i, \sigma_i)$  and  $(\mathbf{r}_j, \sigma_j)$ .  $\mathcal{M}^N$  is the Cartesian product manifold of dimension  $dN$ .

Since the system Hamiltonian can be written as  $\hat{\mathbb{H}} = \hat{\mathbb{H}}_{\mathcal{R}}(\mathcal{R}) + \hat{\mathbb{H}}_{\Sigma}(\Sigma)$ , the last term representing the Zeeman coupling, the many-body wave function  $\Psi(\mathcal{R}, \Sigma)$  can be expressed as a tensor product of a coordinate and a spin function (or a linear combination of such products),

$$\Psi(\mathcal{R}, \Sigma) = \Phi(\mathcal{R}) \otimes \Xi(\Sigma). \quad (8)$$

We want to construct  $N$ -fermion eigenstates of  $\hat{\mathbb{H}}$ ,  $\Psi$ , that are also eigenfunctions of the total spin  $S^2$  ( $S = \sum_{i=1}^N s_i$ ),

$$S^2 \Psi(X) = \hbar^2 s(s+1) \Psi(X), \quad (9)$$

and this is always possible since  $[\hat{\mathbb{H}}, S^2] = 0$ . Thus, the configuration part  $\Phi(\mathcal{R})$  must have the right symmetry in order to account for the Pauli principle. It turns out that a coordinate state  $\Phi(\mathbf{r}_1, \dots, \mathbf{r}_k, \mathbf{r}_{k+1}, \dots, \mathbf{r}_N)$  which is symmetrized according to the Young scheme [13] and has total spin  $s = \frac{N}{2} - k$  will be antisymmetric in the variables  $\mathbf{r}_1, \dots, \mathbf{r}_k$ , and antisymmetric in the variables  $\mathbf{r}_{k+1}, \dots, \mathbf{r}_N$ . Moreover,  $\Phi$  possesses the property of Fock's cyclic symmetry,

$$\left( \mathbb{1} - \sum_{j=k+1}^N \hat{P}_{kj} \right) \Phi = 0, \quad (10)$$

where, in this case,  $\hat{P}_{kj}$  refers to the transposition of particle coordinates  $\mathbf{r}_k$  and  $\mathbf{r}_j$ . This last condition is a very useful one for testing the symmetry of a given coordinate function.

*Quantum projection on curved manifolds.* For a given total spin  $s$  we are thus left with the task of solving the stationary many-body Schrödinger equation  $\hat{\mathbb{H}}_{\mathcal{R}}\Phi(\mathcal{R}) = E\Phi(\mathcal{R})$ , where  $\Phi(\mathcal{R}) = \langle \mathcal{R} | \Phi \rangle$  satisfies the symmetry constraint discussed above. In particular, we are interested in the zero temperature properties of this quantum system, i.e. its ground state properties. To this end, we study the Euclidean time evolution of the state  $\Phi$ , i.e. we analytically continue Eq. 6 to imaginary time (Wick rotation,  $t \rightarrow -i\hbar$ )

$$-\partial_t \Phi = [\hat{\mathbb{H}}_{\mathcal{R}} - E_T] \Phi, \quad (11)$$

whose formal solution  $\Phi(t) = \hat{\mathcal{U}}(t) \Phi_T = \exp[-t(\hat{\mathbb{H}}_{\mathcal{R}} - E_T)]\Phi_T$  is used to determine the limiting distribution

$$\Phi_0 \propto \lim_{t \rightarrow \infty} \Phi(t), \quad (12)$$

which is the largest eigenvalue solution of the evolution operator  $\hat{\mathcal{U}}(t)$  compatible with the condition  $\langle \Phi_0 | \Phi_T \rangle \neq 0$ , where  $\Phi_T$  is a parent state and  $E_T$  is a suitable (constant) energy that shifts the zero of the spectrum of  $\widehat{\mathbb{H}}_{\mathcal{R}}$ .

We would like to solve the multidimensional differential equation Eq. 11 using initial value random walks. In this way, starting with an initial population of walkers (whose state space is  $\mathcal{M}^N$ ) distributed according to  $p(\mathcal{R}, t=0) = \Phi_T$  ( $\Phi_T$  must be positive semi-definite), the ensemble is evolved by successive applications of the short (imaginary) time propagator  $\hat{\mathcal{U}}(\tau)$  ( $\tau = t/M$ , and  $M$  is the number of time slices) to obtain the limiting distribution  $\Phi_0$ . Then, we can introduce a “pseudo partition function”

$$\mathcal{Z} = \langle \Phi_T | \hat{\mathcal{U}}(t) | \Phi_T \rangle \quad (13)$$

in terms of which we can determine the ground state energy  $E_0$  as

$$E_0 - E_T = \lim_{t \rightarrow \infty} -\frac{1}{t} \ln \mathcal{Z} . \quad (14)$$

Similarly, other ground state expectation values, e.g.,  $\langle \Phi_0 | \hat{\mathcal{O}} | \Phi_0 \rangle$ , can be obtained as derivatives (with respect to a coupling constant  $J$ ) of a modified pseudo partition function  $\mathcal{Z}_J$  whose evolution operator has a modified Hamiltonian,  $\widehat{\mathbb{H}}_{\mathcal{R}} + J\hat{\mathcal{O}}$ .

In order to reduce statistical fluctuations in the measured quantities (i.e., observables) one can guide the random walk with an approximate wave function,  $\Phi_G$ , which contains as much of the essential physics as possible (including cusp conditions at possible singularities of the potential  $\hat{V}$ ). Then, instead of sampling the wave function  $\Phi(t)$  one samples the distribution  $\tilde{f}(\mathcal{R}, t) = \Phi(t)\Phi_G$  (properly normalized) with the initial time condition  $\tilde{f}(\mathcal{R}, t=0) = \Phi_T\Phi_G$ . Expectation values of operators  $\hat{\mathcal{O}}$  (observables) that commute with the Hamiltonian have a particularly simple form for guided walkers. For instance,

$$\lim_{t \rightarrow \infty} \frac{\langle \Phi_T | \hat{\mathcal{O}} \hat{\mathcal{U}}(t) | \Phi_T \rangle}{\langle \Phi_T | \hat{\mathcal{U}}(t) | \Phi_T \rangle} = \langle \Phi_G^{-1} \hat{\mathcal{O}} \Phi_T \rangle_{\tilde{f}(t \rightarrow \infty)} , \quad (15)$$

where the average  $\langle \mathcal{A} \rangle_{\tilde{f}}$  stands for

$$\langle \mathcal{A} \rangle_{\tilde{f}} = \frac{\int_{\mathcal{M}^N} \omega \tilde{f}(\mathcal{R}, t \rightarrow \infty) \mathcal{A}(\mathcal{R})}{\int_{\mathcal{M}^N} \omega \tilde{f}(\mathcal{R}, t \rightarrow \infty)} , \quad (16)$$

$\tilde{f}(\mathcal{R}, t \rightarrow \infty)$  is the long-time stationary probability of the system, and the (invariant) volume element  $\omega$  is given by the  $dN$ -form

$$\omega = \left[ \prod_{i=1}^N g^{1/2}(i) \right] dx_1^1 \wedge \cdots dx_1^d \wedge \cdots dx_N^d . \quad (17)$$

Remember that in a general metric space the resolution of the identity operator with respect to the spectral family of the position operator is

$$\mathbb{1} = \int_{\mathcal{M}^N} \omega |\mathcal{R}\rangle \langle \mathcal{R}| . \quad (18)$$

It is important to stress that  $\Phi_T$  and the guiding function  $\Phi_G$  can, in principle, be different functions, although most of the practical calculations use the same function. It turns out that this importance sampling procedure is decisive to get sensible results when the potential  $\hat{V}$  presents some singularities.

Notice, however, that the quantum Hamiltonian  $\hat{\mathbb{H}}$  breaks explicitly time-reversal symmetry, meaning that in general  $\Phi$  will be a complex-valued function. Even if  $\Phi$  were real-valued, because it represents a fermion wave function it can acquire positive and negative values (the case where  $\Xi(\Sigma)$  is totally antisymmetric being the exception). Then, it is clear that we cannot in principle interpret  $\Phi$  or  $\tilde{f}$  as a probability density.

For reasons that will become clear later we will be interested in sampling the probability density  $\tilde{f}(\mathcal{R}, t) = |\tilde{f}(\mathcal{R}, t)|$ . The generalized diffusion equation in curved space for the importance-sampled function  $\tilde{f}$  can be derived directly from Eq. 11 with the result

$$\partial_t \tilde{f} = D \sum_{i=1}^N \left[ g^{-1/2}(i) \partial_\mu \left( g^{\mu\nu}(i) g^{1/2}(i) (\partial_\nu \tilde{f} - \tilde{f} F_\nu) \right) \right] - (E_L - E_T) \tilde{f} , \quad (19)$$

where the drift velocity  $F_\nu(\mathcal{R}) = \partial_\nu \ln \Phi_G^2$ , and the “local energy” of the effective (“Fixed-Phase”) Hamiltonian  $\hat{H}_{FP}$  (see Eq. 50 and its derivation) is  $E_L(\mathcal{R}) = \Phi_G^{-1} \hat{H}_{FP} \Phi_G$  with

$$\hat{H}_{FP} = -D\Delta + D \sum_{i=1}^N \left[ (\partial^\mu \chi(\mathcal{R}) - \frac{e}{\hbar c} a^\mu(i)) (\partial_\mu \chi(\mathcal{R}) - \frac{e}{\hbar c} a_\mu(i)) \right] + \hat{V}(\mathcal{R}) , \quad (20)$$

where  $\chi(\mathcal{R})$  is the phase of the many-body state  $\Phi$ , i.e.  $\Phi = |\Phi| \exp[i\chi]$ . The differential equation satisfied by the distribution function  $\tilde{f}$  is formally equivalent to the one describing Brownian motion on a general manifold (including generation and recombination processes), and corresponds to a Kramers-Moyal expansion with exactly two terms. In fact, we can rewrite the equation above as a Fokker-Planck equation for  $dN$  continuous stochastic variables  $\{\mathbf{r}_i\}_{i=1, \dots, N}$

$$\partial_t \tilde{f} = \left\{ \bar{\mathcal{L}}_{FP} - (\bar{E}_L - E_T) \right\} \tilde{f} , \quad (21)$$

where the (time-independent) Fokker-Planck operator  $\bar{\mathcal{L}}_{FP}$  is given by

$$\bar{\mathcal{L}}_{FP} \bullet = \sum_{i=1}^N \left[ \partial_\mu \partial_\nu \left( \bar{D}^{\mu\nu}(i) \bullet \right) - \partial_\mu \left( \bar{D}^\mu(\mathcal{R}) \bullet \right) \right] . \quad (22)$$

The diffusion matrix (contravariant tensor)  $\bar{D}^{\mu\nu}$  and drift  $\bar{D}^\mu$  (which does not transform as a contravariant vector) are given by

$$\bar{D}^{\mu\nu} = D g^{\mu\nu} \quad (23)$$

$$\bar{D}^\mu = \bar{D}^{\mu\nu} F_\nu + \partial_\nu \bar{D}^{\mu\nu} - \bar{D}^{\mu\nu} \Gamma_{\nu\sigma}^\sigma , \quad (24)$$

where  $\Gamma_{\mu\nu}^\sigma$  is the Christoffel symbol of the second kind

$$\Gamma_{\mu\nu}^\sigma = \frac{1}{2} g^{\sigma\rho} (\partial_\mu g_{\nu\rho} + \partial_\nu g_{\mu\rho} - \partial_\rho g_{\mu\nu}) \quad (25)$$

$$\Gamma_{\nu\sigma}^\sigma = \frac{1}{2} \partial_\nu \ln g , \quad (26)$$

and the modified local energy

$$\bar{E}_L = E_L + \bar{D}^{\mu\nu} \Gamma_{\mu\sigma}^\sigma F_\nu + \partial_\mu \left( \bar{D}^{\mu\nu} \Gamma_{\nu\sigma}^\sigma \right) . \quad (27)$$

Notice, however, that singularities in the “quantum corrections” [14] to the local energy  $E_L$  due to the metric, can induce very large fluctuations in  $\bar{E}_L$ . Moreover, the probability density  $\bar{f}$  does not transform as a scalar function ( $\bar{f}(\mathcal{R}, t) \bar{\omega} = \bar{f}(\mathcal{R}', t) \bar{\omega}'$ , where the primes represent the transformed coordinates and  $\bar{\omega} = dx_1^1 \wedge \cdots dx_1^d \wedge \cdots dx_N^d$  is a volume element in  $\mathcal{M}^N$ ). Therefore, it is more convenient to work with a probability density that is a scalar and which is defined as

$$f(\mathcal{R}, t) = \left[ \prod_{i=1}^N g^{1/2}(i) \right] \bar{f}(\mathcal{R}, t) . \quad (28)$$

The differential equation  $f$  satisfies is of the form Eq. 21 with bar quantities replaced by unbar ones (e.g.  $\bar{\mathcal{L}}_{\text{FP}} \rightarrow \mathcal{L}_{\text{FP}}$ ). It turns out that  $D^{\mu\nu} = \bar{D}^{\mu\nu}$  and the drift (which is not a tensor)

$$D^\mu = D^{\mu\nu} F_\nu + \partial_\nu D^{\mu\nu} + D^{\mu\nu} \Gamma_{\nu\sigma}^\sigma . \quad (29)$$

Note that in this case the quantum correction to the local energy vanishes. Furthermore, if the metric is diagonal, i.e.  $g_{\mu\nu} = g^{1/2} \delta_{\mu\nu}$ , then the correction to the flat space drift also vanishes, i.e.  $\partial_\nu D^{\mu\nu} + D^{\mu\nu} \Gamma_{\nu\sigma}^\sigma = 0$ , and  $D^\mu = D g^{-1/2} F^\mu$ . This last remark is quite important, specially for  $d = 2$  where it is *always* possible to choose a coordinate system ( $\mathbf{r}_i = (\xi_i^1, \xi_i^2)$ ) where the metric tensor is diagonal (conformal gauge [15]), and use the conformal parameterization ( $z_i = \xi_i^1 + i\xi_i^2, \bar{z}_i = \xi_i^1 - i\xi_i^2$ ) which greatly simplifies the resulting expressions (see Section V).

### III. PATH INTEGRAL SOLUTIONS

The generalized Fokker-Planck Eq. 21 describes the time evolution of a distribution function  $f$  which is completely determined by the distribution function at  $t = t_0 = 0$ . In this sense it describes a continuous stochastic process that is Markovian. Because it represents a Markov process, the conditional probability that if the system is in  $\mathcal{R}$  at time  $t = 0$  it will jump to  $\mathcal{R}'$  in time  $t$  (importance-sampled Green’s function)  $G(\mathcal{R} \rightarrow \mathcal{R}'; t)$  contains the complete information about the process, and it follows that the probability densities  $f(\mathcal{R}, t + \tau)$  and  $f(\mathcal{R}, t)$  are connected by

$$f(\mathcal{R}', t + \tau) = \int_{\mathcal{M}^N} \omega G(\mathcal{R} \rightarrow \mathcal{R}'; \tau) f(\mathcal{R}, t) , \quad (30)$$

where the Green’s function  $G(\mathcal{R} \rightarrow \mathcal{R}'; \tau)$  is a transition probability for moving particles from  $\mathcal{R}$  to  $\mathcal{R}'$  in time  $\tau$  with the initial value  $G(\mathcal{R} \rightarrow \mathcal{R}'; 0) = \left[ \prod_{i=1}^N g^{-1/2}(i) \right] \delta(\mathcal{R} - \mathcal{R}')$ , and is formally given by

$$G(\mathcal{R} \rightarrow \mathcal{R}'; \tau) = \tilde{\Phi}_G(\mathcal{R}') \langle \mathcal{R}' | \exp[-\tau(\hat{H}_{FP} - E_T)] | \mathcal{R} \rangle \tilde{\Phi}_G^{-1}(\mathcal{R}) , \quad (31)$$

with



$$\tilde{\Phi}_G(\mathcal{R}) = \left[ \prod_{i=1}^N g^{1/2}(\mathbf{r}_i) \right] \Phi_G(\mathcal{R}) . \quad (32)$$

Path integral solutions for  $f$  may be derived from the transition probability density for small  $\tau$ . Iteration of the Chapman-Kolmogorov equation for  $G$  allows one to express the evolution of  $f(\mathcal{R}', t)$  from the initial distribution  $f(\mathcal{R}, t = 0)$  in terms of the short-time Green's function as

$$f(\mathcal{R}', t) = \int_{\mathcal{M}^N} \omega_{M-1} \cdots \int_{\mathcal{M}^N} \omega_0 G(\mathcal{R}_{M-1} \rightarrow \mathcal{R}_M; \tau) \cdots G(\mathcal{R}_0 \rightarrow \mathcal{R}_1; \tau) f(\mathcal{R}_0, 0) , \quad (33)$$

where  $t = M\tau$ ; we identify  $\mathcal{R}_0 = \mathcal{R}$  and  $\mathcal{R}_M = \mathcal{R}'$ . By simple inspection the solution of the generalized Fokker-Planck equation  $f$  stays positive if it was initially positive (i.e., if  $f(\mathcal{R}, 0) > 0$ .)

It is clear then that the functional integral representation of  $f$  requires knowledge of the infinitesimal evolution operator. It is well-known in a similar context [11] that the integrand of the functional integral is not unique, it is discretization dependent (compatible with the Markovian property of the paths since  $\mathcal{R}(t)$  is only sampled at  $t - \tau$  and  $t$ .) On the other hand, it is crucial for numerically simulating those paths to use a discretization where the drift velocity and diffusion are evaluated at the **prepoint** in the integral equation. Following Feynman [16] we have determined the functional form of  $G(\mathcal{R} \rightarrow \mathcal{R}'; \tau)$  to  $\mathcal{O}(\tau^2)$ . We are going to present the final result and omit the details of the calculation which are just simple (although lengthy) manipulations of Taylor series expansions and gaussian integration. Thus, to  $\mathcal{O}(\tau^2)$  the short-time conditional probability is given by

$$G(\mathcal{R} \rightarrow \mathcal{R}'; \tau) = G_b(\mathcal{R} \rightarrow \mathcal{R}'; \tau) \prod_{i=1}^N G_i^0(\mathcal{R} \rightarrow \mathcal{R}'; \tau) \quad (34)$$

where

$$G_b(\mathcal{R} \rightarrow \mathcal{R}'; \tau) = \exp \left[ -\tau \left( \frac{[E_L(\mathcal{R}) + E_L(\mathcal{R}')] }{2} - E_T \right) \right] , \quad (35)$$

and

$$G_i^0(\mathcal{R} \rightarrow \mathcal{R}'; \tau) = \left( \frac{1}{4\pi D\tau} \right)^{d/2} \exp \left[ -\frac{(x_i'^\mu - x_i^\mu - \tau D^\mu(\mathcal{R})) g_{\mu\nu}(\mathbf{r}_i) (x_i'^\nu - x_i^\nu - \tau D^\nu(\mathcal{R}))}{4D\tau} \right] , \quad (36)$$

that is, a gaussian distribution with variance matrix  $2D^{\mu\nu}$  and mean  $x_i^\mu + \tau D^\mu(\mathcal{R})$ . Sample trajectories (continuous but nowhere differentiable) are generated by using the Langevin equation associated with the process, i.e.  $x_i'^\mu = x_i^\mu + \tau D^\mu(\mathcal{R}) + \sqrt{\tau} \eta$ , where  $\eta$  is a gaussian random variable with zero mean. Note that  $D^\mu$  and  $D^{\mu\nu}$  are evaluated at the **prepoint** in the integral equation.

Therefore, the Wick-rotated path integral for  $G(\mathcal{R} \rightarrow \mathcal{R}'; t)$  is

$$G(\mathcal{R} \rightarrow \mathcal{R}'; t) = \int_{\mathcal{R}(0)=\mathcal{R}}^{\mathcal{R}(t)=\mathcal{R}'} \mathcal{D}[\omega(t)] \exp[-S[\mathcal{R}(t)]] , \quad (37)$$

where the measure  $\mathcal{D}[\omega(t)] = \lim_{M \rightarrow \infty} (4\pi D\tau)^{-Md/2} \omega_1 \cdots \omega_{M-1}$ , and the Euclidean action

$$S[\mathcal{R}(t)] = \int_0^t dt' \left\{ \frac{1}{4D} \sum_{i=1}^N (\dot{x}_i^\mu - D^\mu[\mathcal{R}(t')]) g_{\mu\nu}(i) (\dot{x}_i^\nu - D^\nu[\mathcal{R}(t')]) + E_L[\mathcal{R}(t')] - E_T \right\} . \quad (38)$$

The integrand above represents a generalized Onsager-Machlup function [17], and the dot is a short-hand for time derivatives. In closing this Section, we would like to mention that functional integral solutions for  $\bar{f}$  can be obtained from previous expressions after making the replacement  $(D^\mu, E_L) \rightarrow (\bar{D}^\mu, \bar{E}_L)$ .

*Interpretation of the quantum corrections.* The general methodology we have developed so far, can be equally applied to other situations which do not necessarily involve a curved manifold such as, for instance, particles moving in a medium with position dependent diffusion constant. In order to adapt our previous formalism, we need to understand qualitatively the origin of the quantum corrections to the short-time propagator obtained above. To this end, we will illustrate the general idea with the following 1d equation ( $\mathcal{M} = \mathbb{R}$ ,  $N = 1$ )

$$\partial_x^2(D(x)f(x,t)) = \partial_t f(x,t) . \quad (39)$$

The “standard” approach to finding the Green’s function for this problem is simply to solve the equation  $\partial_x^2(D(x)G(x,t)) = \partial_t G(x,t)$  subject to the boundary condition  $G(x,0) = \delta(x)$ . We can do this by taking the Fourier transform in  $x$ :

$$- \frac{k^2}{2\pi} \int_{\mathcal{M}} dk' D(k-k') G(k',t) = \partial_t G(k,t) , \quad (40)$$

with the boundary condition  $G(k,0) = 1$ . This is more complex than the usual diffusion equation because we get a convolution of  $D(k)$  and  $G(k,t)$ . However, we can find an approximate solution for  $G(k,t)$ , valid for small time, by noting that the boundary condition implies that, for small times  $t$ ,  $G(k,t) - G(k',t) \sim \mathcal{O}(t)$  and so we have

$$- \frac{k^2}{2\pi} \int_{\mathcal{M}} dk' D(k-k') G(k,t) + \mathcal{O}(t) = \partial_t G(k,t) \quad (41)$$

or, simply,  $-k^2 D(x=0)G(k,t) + \mathcal{O}(t) = \partial_t G(k,t)$ , where  $D(x=0)$  is  $D(x)$  evaluated at the **prepoint**. For small times we can ignore the order  $t$  term and solve for  $G$  with the result  $G(k,t) = \exp[-t k^2 D(0)]$ . Taking the inverse Fourier transform we finally have

$$G(x,t) = \frac{1}{\sqrt{4\pi D(0)t}} \exp[-x^2/4D(0)t] + \mathcal{O}(t^2) , \quad (42)$$

which is just the plain Green’s function for a 1d random-walk with  $D(x)$  evaluated at the **prepoint** and with **no quantum corrections**. This is, in fact, the result that the Green’s function for the Jacobian times  $\bar{f}$  has no quantum corrections.

To make things clear let us look at a different equation with the same boundary conditions

$$D(x)\partial_x^2 G(x,t) = \partial_t G(x,t) , \quad (43)$$

which characterizes a free Brownian particle in 1d. Again, taking the Fourier transform we get

$$-\frac{1}{2\pi} \int_{\mathcal{M}} dk' k'^2 D(k-k') G(k', t) = \partial_t G(k, t) . \quad (44)$$

Making the same approximation as above, replacing  $G(k', t)$  with  $G(k, t)$  in the integrand, making an error of  $\mathcal{O}(t)$ , and noticing that

$$\frac{1}{2\pi} \int_{\mathcal{M}} dk' (k-k')^2 D(k') = k^2 D(0) + 2ki \partial_x D(0) - \partial_x^2 D(0) \quad (45)$$

we get  $G(k, t) = \exp[-t (k^2 D(0) + 2ki \partial_x D(0) - \partial_x^2 D(0))]$ . When we take the inverse Fourier transform the terms with derivatives of  $D(x)$  at  $x = 0$  give precisely the quantum corrections for this simple case

$$G(x, t) = \frac{1}{\sqrt{4\pi D(0)t}} \exp[-(x - 2t\partial_x D(0))^2 / 4D(0)t + t \partial_x^2 D(0)] + \mathcal{O}(t^2) . \quad (46)$$

This is the result that the Green's function for  $\bar{f}$  has quantum corrections.

The general case is just as simple, and the following rule emerges. Given any second order differential equation (first order in  $t$ ), no matter how many dimensions, with or without curvature, with or without a position dependent diffusion constant, the rule for obtaining the short-time Green's function with everything evaluated at the prepoint is as follows: **Bring all derivatives in each term all the way to the left of that term.** Once this is done one can simply write down the Green's function for a generalized diffusion process assuming the  $D(x)$ ,  $D^\mu$ ,  $D^{\mu\nu}$ , whatever position dependent terms they may be, are constant and evaluated at the prepoint. The quantum corrections are then seen to be simply those extra terms we get when commuting the derivatives to the left.

*Fermion-phase problem: Fixed-Phase method.* It is evident that one cannot make a probability density out of a complex and/or antisymmetric wave function. This is the reason why we decided to write down Fokker-Planck equations for the distribution  $f$  (or  $\bar{f}$ ) and not  $\tilde{f}$ . Nevertheless, the phase factor associated with the original complex distribution must show up in the evaluation of the expectation values. It is well-known that this causes the variance of the computed results to increase exponentially with increasing number of degrees of freedom. This problem is known as the fermion-phase [18] catastrophe, and in this Section we will review a method [7] to obtain stable, albeit approximate, path-integral solutions whose stochastic determination has a polynomial, instead of exponential, complexity. The generalization of the ideas presented below to bosons (with complex-valued states) or anyons in general is straightforward [19].

In order to avoid cumbersome notation which would obscure the main ideas, here we will consider a simplified version of our original Hamiltonian

$$\widehat{\mathbb{H}}_{\mathcal{R}} = \frac{\boldsymbol{\Pi} \cdot \boldsymbol{\Pi}}{2m^*} + \widehat{V}(\mathcal{R}) , \quad (47)$$

where, for simplicity, we introduced the vector notation,  $\boldsymbol{\Pi} = (\Pi(1), \dots, \Pi(N))$ , and in this subsection the same convention will be used for other bold quantities. The microscopic equations governing the imaginary-time evolution of our interacting system can be found from a variational principle of the form  $\delta S[\mathcal{R}(t)] = 0$ , where the Euclidean action is given by

$$S[\mathcal{R}(t)] = \int_0^t dt' \int_{\mathcal{M}^N} \omega \left\{ \frac{1}{2m^*} [\mathbf{\Pi}\Phi]^* \cdot [\mathbf{\Pi}\Phi] + \hat{V} \Phi^* \Phi + \Phi^* \partial_{t'} \Phi \right\}. \quad (48)$$

Finding the states  $\Phi$  and  $\Phi^*$  which minimize  $S[\mathcal{R}(t)]$  is equivalent to solving the Schrödinger equation and its complex conjugate. Equivalently, we can consider as independent real fields the phase and modulus of the wave function, i.e.  $|\Phi|$  and  $\chi$  such that  $\Phi = |\Phi| \exp[i\chi]$ , and perform independent functional variations on  $S[\mathcal{R}(t)]$ . The resulting Euler-Lagrange equations are:

$$\begin{cases} -\partial_t |\Phi| = \Re \left\{ \exp[-i\chi] \widehat{\mathbf{H}}_{\mathcal{R}} \Phi \right\} & = \hat{H}_{FP} |\Phi| \\ -(\partial_t \chi) |\Phi|^2 = \Im \left\{ \exp[-i\chi] \widehat{\mathbf{H}}_{\mathcal{R}} \Phi \right\} |\Phi| & = -\frac{\hbar}{2} \boldsymbol{\partial}_{\boldsymbol{\mu}} \cdot \mathbf{J}^{\boldsymbol{\mu}} \end{cases}, \quad (49)$$

where  $\Re$  and  $\Im$  stand for the real and imaginary parts of the expressions in brackets, respectively,

$$\hat{H}_{FP} = \frac{\mathbf{p} \cdot \mathbf{p}}{2m^*} + \tilde{V}(\mathcal{R}), \quad \tilde{V} = \hat{V} + D \left( \partial^\mu \chi(\mathcal{R}) - \frac{e}{\hbar c} \mathbf{a}^\mu \right) \cdot \left( \partial_\mu \chi(\mathcal{R}) - \frac{e}{\hbar c} \mathbf{a}_\mu \right), \quad (50)$$

and

$$\mathbf{J}^\mu = \frac{1}{2m^*} (\Phi^* [\mathbf{\Pi}^\mu \Phi] + [\mathbf{\Pi}^\mu \Phi]^* \Phi) = \frac{|\Phi|^2}{m^*} \left( \hbar \boldsymbol{\partial}_\mu \chi(\mathcal{R}) - \frac{e}{c} \mathbf{a}_\mu \right) \quad (51)$$

is the probability current. The singularities of  $\chi(\mathcal{R})$  occur at the zeros of  $\Phi$ , which generically have codimension two.

So far we have simply mapped the original fermion problem into a bosonic one for  $|\Phi|$  but still coupled to its phase fluctuations. Alternatively, one can regard this as a gauge transformation of the original fermion problem, whose effect is to add a non-local gauge field potential,  $\partial^\mu \chi$ , giving rise to a *fictitious* magnetic field. Notice that it is this gauge field that contains information on particle statistics. Moreover, although the geometry of  $\chi(\mathcal{R})$  can be altered by a gauge transformation, the singularities remain invariant.

The Fixed-Phase (FP) method [7] consists in making a choice for the phase,  $\chi_T$ , and solving the bosonic problem for  $|\Phi|$  *exactly* using stochastic methods. The method is *stable* and has the property of providing a variational upper bound to the exact ground energy  $E_0$ ,  $E_{FP} \geq E_0$  (the equality holds when  $\chi_T$  is the exact ground state phase), and for a given  $\chi_T$  the lowest energy consistent with this phase. The trial phases  $\chi_T$  should conserve the symmetries of  $\widehat{\mathbf{H}}_{\mathcal{R}}$  and particle statistics (for time-reversal invariant systems there is a way for systematically improving a given mean-field phase using projection techniques [20]). Notice that the FP method projects out the lowest energy state of a given symmetry. Therefore, the method allows one to compute also excitations which are “ground states” of a particular symmetry. For ground state properties of real symmetric Hamiltonian operators the FP approach reduces [7] to the Fixed-Node method [21].

#### IV. COMPUTATIONAL IMPLEMENTATION

In this Section we present an algorithm for computing the ground state properties of quantum many-body systems defined on a curved manifold with general metric  $g^{\mu\nu}$ . As

mentioned in the Introduction, this can be accomplished by performing all multidimensional integrals using Monte Carlo techniques. In this way, ground state expectation values are obtained by averaging over a large number of particle configurations generated according to a certain limiting probability distribution  $p(\mathcal{R}, t \rightarrow \infty)$ . There is some freedom in the choice of this distribution  $p(\mathcal{R}, t)$ , however, to reduce statistical fluctuations in the observables to be computed it is more efficient to use the so-called *importance-sampled* distribution  $\bar{f}(\mathcal{R}, t)$ , which is the product of the absolute value of the solution of the time dependent Schrödinger equation  $\Phi(\mathcal{R}, t)$  and some positive function  $\Phi_G(\mathcal{R})$  that is the best available approximation to the modulus of the ground state eigenfunction. In a curved manifold, on the other hand, it is more convenient to work with the *modified importance-sampled* distribution  $f(\mathcal{R}, t)$ , which is defined as a product of the conventional importance-sampled distribution  $\bar{f}(\mathcal{R}, t)$  and the metric (see Eq. 28).

The propagation of particle configurations in time  $\tau$  is determined by the conditional probability (Green's function)  $G(\mathcal{R} \rightarrow \mathcal{R}'; \tau)$ , whose separation into a diffusion (plus drift) and branching parts (see Eq. 34) makes it very simple to simulate numerically. The gaussian term represents propagation according to the equation  $x_i'^\mu = x_i^\mu + \tau D^\mu(\mathcal{R}) + \sqrt{\tau} \eta$ , where  $\eta$  is a gaussian random variable with zero mean. The effect of the term  $\tau D^\mu(\mathcal{R})$  is to superimpose a drift velocity on the random diffusion process so that particle configurations are directed towards regions of configuration space where  $\Phi_G(\mathcal{R})$  is large. The branching term  $G_b(\mathcal{R} \rightarrow \mathcal{R}'; \tau)$  in Eq. 35, determines the creation and annihilation of configurations (walkers) at the point  $\mathcal{R}'$  after a move. If the size of the ensemble of walkers at any time  $t$  is defined as

$$\mathcal{P}(t) = \int_{\mathcal{M}^N} \bar{\omega} f(\mathcal{R}, t) \quad (52)$$

then, its rate of change is given by

$$\partial_t \mathcal{P}(t) = - \int_{\mathcal{M}^N} \bar{\omega} [E_L(\mathcal{R}) - E_T] f(\mathcal{R}, t) . \quad (53)$$

Therefore, if the local energy  $E_L(\mathcal{R})$  is a smooth function of  $\mathcal{R}$ , and the trial energy  $E_T$  is suitably adjusted, the size of the ensemble of walkers will remain approximately constant as the configurations propagate. In particular, if the local energy is constant and equal to  $E_T$  then the fluctuations in the ensemble size will vanish. To ease notation, in the rest of the paper we will only consider the standard situation  $\Phi_T = \Phi_G$ . In such a case, ground state expectation values of a generic observable  $\hat{O}$  will be computed as

$$\lim_{t \rightarrow \infty} \frac{\langle \Phi_G | \hat{O} \hat{U}(t) \Phi_G \rangle}{\langle \Phi_G | \hat{U}(t) \Phi_G \rangle} = \langle \Phi_G^{-1} \hat{O} \Phi_G \rangle_{f(t \rightarrow \infty)} = \int_{\mathcal{M}^N} \bar{\omega} \frac{f(\mathcal{R}, t \rightarrow \infty)}{\mathcal{P}(t \rightarrow \infty)} [\Phi_G^{-1} \hat{O} \Phi_G](\mathcal{R}) . \quad (54)$$

In the following we present a step by step computational algorithm for implementing the stochastic approach discussed above. Most parts of the algorithm follow closely the standard DMC method, described for instance in [21], but we believe that it is useful to present these steps in detail here because a number of straightforward but subtle modifications due to the space curvature are involved. To be more specific (without losing the general features), let us present the algorithm as it is applied to fermionic systems within the FP approach.

*Algorithm.*

§ 1. Construct a guiding wave function  $\Phi_G$ , which is the best available approximation to the exact ground state (or lowest energy state of a given symmetry). In principle any choice of  $\Phi_G$  which has finite overlap with the exact state is acceptable, but the more accurate  $\Phi_G$  is the faster the convergence to the stationary solution will be, and the lower the statistical fluctuations will be as well. Recall that zero variance is obtained when the guiding wave function is equal to the desired ground state (and the ground state is bosonic).

§ 2. Given the guiding function compute the quantum drift velocity  $F_\nu = \partial_\nu \ln \Phi_G^2$  and the local energy  $E_L = \Phi_G^{-1} \hat{H}_{FP} \Phi_G$ , where  $\hat{H}_{FP}$  is the FP Hamiltonian defined in Eq. 20.  $F_\nu$  is used to construct the drift vector  $D^\nu$  according to Eq. 29, and the drift and local energy are used in evaluating the short-time Green's function according to Eqs. 34, 35, and 36. When a simple guiding function can be constructed, the expressions for the drift and the local energy can be evaluated analytically, but in most cases this must be done numerically.

§ 3. A set of  $N_w$  initial configurations or walkers  $\{\mathcal{R}_j(t=0)\}$  ( $j = 1, \dots, N_w$ ) is created, such that particles in each walker are distributed according to the *modified importance-sampled* distribution  $f(\mathcal{R}, t=0) = [\prod_{i=1}^N g^{1/2}(i)] |\Phi_G|^2$  (which is equivalent to using the Variational Monte Carlo (VMC) technique).

§ 4. Each walker  $\mathcal{R}_j$  is diffused for a time  $\tau$  according to the gaussian part of the propagator  $\prod_{i=1}^N G_i^0(\mathcal{R}_j \rightarrow \mathcal{R}'_j; \tau)$ . This can be accomplished by moving each particle coordinate  $x_i^\mu$  according to

$$x_i'^\mu = x_i^\mu + \tau D^\mu(\mathcal{R}_j) + \sqrt{\tau} \eta , \quad (55)$$

where  $\eta$  is a Gaussian random variable with a mean of zero and a variance of  $2D^{\mu\nu} = 2Dg^{\mu\nu}$ .

§ 5. The move from  $\mathcal{R}_j$  to  $\mathcal{R}'_j$  is then accepted with a probability

$$A(\mathcal{R}_j \rightarrow \mathcal{R}'_j; \tau) \equiv \min(1, W(\mathcal{R}_j, \mathcal{R}'_j; \tau)) , \quad (56)$$

where

$$W(\mathcal{R}, \mathcal{R}'; \tau) \equiv \left[ \prod_{i=1}^N \frac{g(\mathbf{r}'_i)}{g(\mathbf{r}_i)} \right] \left| \frac{\Phi_G(\mathcal{R}')}{\Phi_G(\mathcal{R})} \right|^2 \frac{G(\mathcal{R}' \rightarrow \mathcal{R}; \tau)}{G(\mathcal{R} \rightarrow \mathcal{R}'; \tau)} . \quad (57)$$

This step ensures detailed balance in the Monte Carlo procedure. A typical acceptance ratio is in excess of 99%. Notice that if  $G(\mathcal{R} \rightarrow \mathcal{R}'; \tau)$  is the exact Green's function, and not its short-time approximation, then  $W$  is unity and this step is not necessary. This is because the Green's function of an Hermitian operator is symmetric, i.e.  $G(\mathcal{R} \rightarrow \mathcal{R}'; \tau) = G(\mathcal{R}' \rightarrow \mathcal{R}; \tau)$ , but this is not the case for any importance-sampled distribution function equation.

§ 6. After all the particles of a given walker have been diffused from the initial position  $\mathcal{R}_j$  to the position  $\mathcal{R}'_j$  and the move is accepted, then the values of the drift  $D^\mu$ , the local energy  $E_L$ , and  $\Phi_G$  are updated. We could have equally well move all particles at once in step 4 before step 5, however, the acceptance probability for a given time step is reduced considerably. Depending upon the particular problem one can adopt one of the two strategies: single or multiparticle moves.

§ 7. The multiplicity (weight)  $M$  of a given walker, is computed from the branching part of the Green's function Eq. 35

$$M = G_b(\mathcal{R} \rightarrow \mathcal{R}'; \tau_a) , \quad (58)$$

where  $\tau_a \leq \tau$  because some of the moves can be rejected. If the mean-squared distance the particles would diffuse in the absence of the rejection step is  $\langle r^2 \rangle_{tot}$ , and the actual mean-squared distance is  $\langle r^2 \rangle_a$  then the actual time used in a branching step  $\tau_a = \tau \langle r^2 \rangle_a / \langle r^2 \rangle_{tot}$ . In the case of multiparticle moves, the effective time step must be calculated separately from a computation of the accepted to attempted moves. Since  $\mathbf{M}$  is, in general, not an integer one can use instead the integer

$$\hat{\mathbf{M}} = \text{int}(\mathbf{M} + \xi) ,$$

where  $\xi$  is a random number uniform in the range  $[0, 1]$ . In this case the average density of walkers is conserved and  $\langle \hat{\mathbf{M}} \rangle = \mathbf{M}$ . If  $\hat{\mathbf{M}} = 0$  then the walker is deleted from the ensemble; otherwise  $\hat{\mathbf{M}} - 1$  copies of the configuration are made and added to the ensemble. Note that fixing  $\hat{\mathbf{M}} = 1$  is equivalent to eliminate branching and, consequently, to perform a VMC calculation with limiting distribution  $f(\mathcal{R}, t \rightarrow \infty) = [\prod_{i=1}^N g^{1/2}(i)] |\Phi_G|^2$ .

§ 8. After diffusing and branching all walkers in time  $\tau$  the mean value of the local energy over all walkers is computed from the obtained distribution. One has to start averaging over these values, after some target (equilibration) time, when the configurations are sampled according to the limiting stationary distribution  $f(\mathcal{R}, t \rightarrow \infty)$ . The target time depends upon the particular problem and how close  $\Phi_G$  is to the exact state.

§ 9. Using the average value of the local energy over the whole ensemble of walkers  $\langle E_L(\mathcal{R}) \rangle_{f(t \rightarrow \infty)}$ , the trial energy  $E_T$  is updated according to  $E_T = (E_T + E_L)/2$ . Mixing this estimate with an old value of the trial energy, allows one to improve the convergence.

§ 10. After computing the average energy over a sufficiently long time ( $\tau N_m$ , where  $N_m$  is the number of moves per configuration), its value is stored and the first block is completed.  $N_m$  should be large enough for there to be little statistical correlation between energy subaverages obtained in different blocks. A new ensemble of  $N_w$  walkers is generated by randomly copying or deleting configurations, and steps 4 to 9 are repeated completing another block. One has to do as many blocks as it takes in order to reach the desired statistical accuracy. Notice, however, that because the propagator is only accurate to  $\mathcal{O}(\tau^2)$ , the distribution  $f(\mathcal{R}, t \rightarrow \infty)$  and the resulting estimates will have a time step bias. The way to eliminate this bias is by extrapolating all computed expectation values to  $\tau \rightarrow 0$ .

Figure 1 shows a schematic flow diagram of the algorithm presented in this Section.

## V. EXAMPLE: ELECTRON-MONOPOLE IN $S^2$

As an example application of the method we have developed in the previous Sections we consider the problem of a single particle of charge  $e$ , mass  $m^*$  and vector position  $\mathbf{r} = (x^1, x^2, x^3)$  in  $\mathbb{R}^3$  confined to the surface of a sphere of radius  $R$  centered at the origin ( $\mathcal{M} = S^2$ ,  $N = 1$ ) moving in the presence of the vector potential of a Dirac monopole at the origin. This problem can be solved in closed form and so constitutes an ideal model system for testing the accuracy of the stochastic solutions we can derive using the formalism developed in previous Sections. Moreover, the case of  $N$  interacting electrons confined to  $S^2$  in the presence of a monopole field serves as the basic model which captures the essential physics of the quantum Hall effect [22].

The Pauli Hamiltonian for a spinless particle in  $S^2$  is

$$\widehat{\mathbb{H}}_{\mathcal{R}} = \frac{|\hat{\mathbf{r}} \wedge (-i\hbar\nabla - (e/c) \mathbf{A})|^2}{2m^*}, \quad (59)$$

where  $\hat{\mathbf{r}} = \mathbf{r}/R$ , and  $\mathbf{A}$  is the monopole vector potential ( $\nabla \wedge \mathbf{A} = B \hat{\mathbf{r}}$ ,  $B$  being the strength of the radial field.) Therefore, the total number of flux quanta  $2\mathcal{S}$  piercing the surface of the sphere is given by  $2\mathcal{S} = 4\pi R^2 B/\phi_0$ , where  $\phi_0 = hc/|e|$  is the elementary flux quantum. Following Wu and Yang [23] we can construct angular momentum operators  $\mathbf{L} = \mathbf{r} \wedge (-i\hbar\nabla - (e/c) \mathbf{A}) + \hbar\mathcal{S} \hat{\mathbf{r}}$  in terms of which the Hamiltonian reads

$$\widehat{\mathbb{H}}_{\mathcal{R}} = \frac{|\mathbf{L}|^2 - \hbar^2 \mathcal{S}^2}{2m^* R^2}. \quad (60)$$

If we choose a gauge where the vector potential is  $\mathbf{A} = -BR \cot \theta \hat{\varphi}$ , then the Hamiltonian, Eq. 60, can be written as

$$\widehat{\mathbb{H}}_{\mathcal{R}} = \frac{D}{R^2} \left[ -\partial_\theta^2 - \frac{1}{\sin^2 \theta} \partial_\varphi^2 - \cot \theta \partial_\theta + 2i\mathcal{S} \frac{\cot \theta}{\sin \theta} \partial_\varphi + \mathcal{S}^2 \cot^2 \theta \right], \quad (61)$$

in terms of the usual spherical angles  $\theta$  and  $\varphi$  ( $0 \leq \theta \leq \pi$ ,  $0 \leq \varphi < 2\pi$ , see Fig. 2.) The eigenstates of this Hamiltonian are monopole harmonics (normalized to 1) [23]

$$\begin{aligned} Y_{\mathcal{S},n,m} &= \mathcal{N}_{\mathcal{S}nm} (-1)^{\mathcal{S}+n-m} \exp[-i\mathcal{S}\varphi] u^{\mathcal{S}+m} v^{\mathcal{S}-m} \mathcal{F}(|u|, |v|), \\ \mathcal{F}(|u|, |v|) &= \sum_{k=0}^n (-1)^k \binom{n}{k} \binom{2\mathcal{S}+n}{\mathcal{S}+n-m-k} (v\bar{v})^{n-k} (u\bar{u})^k, \\ \mathcal{N}_{\mathcal{S}nm} &= \left( \frac{2\mathcal{S}+2n+1}{4\pi} \frac{(\mathcal{S}+n-m)! (\mathcal{S}+n+m)!}{n! (2\mathcal{S}+n)!} \right)^{1/2}, \end{aligned} \quad (62)$$

where  $u = \cos(\theta/2) \exp[i\varphi/2]$  and  $v = \sin(\theta/2) \exp[-i\varphi/2]$  are spinor coordinates,  $n$  is the Landau level quantum number, and  $m = -\mathcal{S}-n, -\mathcal{S}-n+1, \dots, \mathcal{S}+n$  is the ( $L_{x^3}$ ) angular momentum quantum number which labels degenerate states within the  $n^{\text{th}}$  level. In the sum above the binomial coefficient  $\binom{\alpha}{\beta}$  vanish when  $\beta > \alpha$  or  $\beta < 0$ . For a given  $\mathcal{S}$  and  $m$ , the ground state ( $n=0$ ) and first excited state ( $n=1$ ) are

$$\psi_{gs} \propto u^{\mathcal{S}+m} v^{\mathcal{S}-m}, \quad (63)$$

$$\psi_{es} \propto [2(\mathcal{S}+1)v\bar{v} - (\mathcal{S}-m+1)] \psi_{gs}, \quad (64)$$

respectively. The energy of a state with Landau level quantum number  $n$  is given by

$$E_n = \left( 2n+1 + \frac{n(n+1)}{\mathcal{S}} \right) \frac{\hbar\omega_c}{2}, \quad (65)$$

where  $\omega_c$  is the cyclotron frequency ( $\omega_c = |e|B/m^*c$ ).

Let us now reformulate the electron-monopole problem in a way consistent with the notations introduced in the previous Sections. In this way one can compare the exact result to the numerical one obtained with the algorithm developed in this paper, thus testing the numerical technique. First, instead of the spherical angles  $\theta$  and  $\phi$  we introduce new coordinates  $z$  and  $\bar{z}$ , where  $z = \tan(\theta/2) \exp[-i\varphi]$ , and  $\bar{z}$  is its complex conjugate. Geometrically,



this transformation can be viewed as a stereographic projection of the sphere onto the plane, as illustrated in Fig. 2. The Hamiltonian can be rewritten as

$$\widehat{\mathbb{H}}_{\mathcal{R}} = \frac{i}{m^*} g^{-1/4} (p_z - \bar{\mathcal{A}}(z)) (p_{\bar{z}} - \mathcal{A}(z)) g^{1/4} + \frac{D\mathcal{S}}{R^2}, \quad (66)$$

in terms of the (non-hermitian) canonical momenta  $p_z$  and  $p_{\bar{z}}$ , and

$$\mathcal{A}(z) = -i \frac{\hbar \mathcal{S}}{2} z \left( \frac{1 - |z|^2}{|z|^2 (1 + |z|^2)} \right), \quad (67)$$

with metric tensor

$$g^{\mu\nu}(z, \bar{z}) = \begin{pmatrix} 0 & \frac{(1+z\bar{z})^2}{2R^2} \\ \frac{(1+z\bar{z})^2}{2R^2} & 0 \end{pmatrix}. \quad (68)$$

Naturally, the particles moving in the projected plane are in a space with curvature, corresponding to that of the sphere. Notice that the metric tensor is diagonal when written in terms of  $(\xi^1, \xi^2)$ , such that  $z = \xi^1 + i \xi^2$ , i.e.  $g^{\mu\nu}(\xi^1, \xi^2) = \frac{(1+|z|^2)^2}{4R^2} \delta^{\mu\nu}$  (i.e, it corresponds to the conformal gauge). Then, the drift is simply  $D_\mu = D F_\mu$ .

The stochastic method developed above allows one to obtain the exact energy eigenvalues of the electron-monopole problem in  $S^2$  iff we know the exact phase of the eigenfunctions. In other words, if the trial state is chosen such that it has the exact ground state phase, then independently of its modulus our stochastic approach will lead to the exact ground state energy. Similarly, if the trial state has a phase corresponding to an excited state eigenfunction then we will obtain the exact excited state energy eigenvalue. In the next two subsections we construct simple trial states for the ground and first excited states of the one particle problem. Their modulus are then used as guiding functions  $\Phi_G$ . Using these trial states we will apply our technique and illustrate the main ideas of our method.

*Ground State ( $n = 0$ ):* The  $2\mathcal{S} + 1$  degenerate ground states of the electron-monopole system are labeled by their  $L_{x^3} = \hbar[\bar{z}\partial_{\bar{z}} - z\partial_z]$  angular momentum quantum numbers  $m = -\mathcal{S}, \dots, \mathcal{S}$ . Here we consider the  $m = \mathcal{S}$  ground state for which the exact (unnormalized) wave function can be written

$$\psi_{gs} = \left( \frac{|z|}{z(1 + |z|^2)} \right)^{\mathcal{S}} \equiv |\psi_{gs}| e^{i\varphi_{gs}}. \quad (69)$$

To illustrate our method we imagine that we do not know this exact ground state  $\psi_{gs}$  but instead we have constructed the following two trial states

$$\psi_{T1} = \left( \frac{|z|}{z(1 + |z|^2)} \right)^{\mathcal{S}} \frac{1}{1 + \lambda|z|^2} \equiv |\psi_{T1}| e^{i\varphi_{T1}}, \quad (70)$$

and

$$\psi_{T2} = \left( \frac{|z|}{z(1 + |z|^2)} \right)^{\mathcal{S}} \left( \frac{|z|}{z} \right)^{\alpha} \equiv |\psi_{T2}| e^{i\varphi_{T2}}, \quad (71)$$

where  $\lambda$  and  $\alpha$  are real valued constants.

The trial states  $\psi_{T1}$  and  $\psi_{T2}$  have been constructed so that for  $\lambda = 0$  and  $\alpha = 0$  they are both equal to the exact ground state,  $\psi_{gs}$ . For  $\lambda \neq 0$ , the modulus of  $\psi_{T1}$  is no longer equal to that of the exact ground state, but the phase of the wave function is *exact*, i.e.

$$|\psi_{T1}| \neq |\psi_{gs}|, \quad \varphi_{T1} = \varphi_{gs}. \quad (72)$$

In contrast, for  $\alpha \neq 0$ , the modulus of  $\psi_{T2}$  is exact, but the phase is approximate,

$$|\psi_{T2}| = |\psi_{gs}|, \quad \varphi_{T2} \neq \varphi_{gs}. \quad (73)$$

It follows that if  $\psi_{T1}$  is used as a trial state in a FP DMC simulation the resulting energy will be the *exact* ground state energy  $E_0 = \hbar\omega_c/2$ , while if  $\psi_{T2}$  is used as a trial state the simulation will not lead to the exact ground state energy, but instead will provide a variational upper bound.

As has already been emphasized the trial state used in a FP DMC simulation should be constructed to be the *best available* approximation to the exact eigenstate, since the quality of the trial state can greatly influence the speed of convergence and the statistical accuracy of the result of the simulation. This can be clearly illustrated by considering the trial state  $\psi_{T2}$ . Since the modulus of  $\psi_{T2}$  is exact the drift velocity  $F$  which depends only on the modulus of the trial state will correspond to the exact drift velocity and in the absence of the branching term will lead to the exact density distribution. It is straightforward to show that

$$F_1 = -\frac{4\mathcal{S} \xi^1}{1 + |z|^2}, \quad F_2 = -\frac{4\mathcal{S} \xi^2}{1 + |z|^2}, \quad (74)$$

where  $F_\mu = \partial_{\xi^\mu} \ln |\psi_{T2}|^2$ , indicating that walkers are guided away from the regions where the wave function is small and, in this way, the particle tends to spend most of the time near the top of the sphere ( $\theta = 0$ ). A potential problem appears when we consider the local energy,

$$E_L = |\psi_{T2}|^{-1} \hat{H}_{FP} |\psi_{T2}| = \frac{\hbar\omega_c}{2} \left[ 1 + \frac{(1 + |z|^2)^2}{\mathcal{S}} \left( \frac{\alpha\mathcal{S}}{1 + |z|^2} + \frac{\alpha^2}{4|z|^2} \right) \right] \quad (75)$$

which, of course, is not exact due to the approximate phase of the trial state. In particular,  $E_L$  *diverges* as  $|z| \rightarrow 0$ . As we have just shown, the drift will tend to push the particle towards  $z = 0$ , leading to large fluctuations in the local energy. This in turn can lead to huge fluctuations in the population size (number of walkers), since the size of the population depends exponentially on the local energy. Thus, in this particular example, one has to take small values for  $\alpha$  ( $\alpha \ll 1$ ) in order to assure fast convergence and good statistical accuracy.

Figure 3 shows the results of FP DMC simulations, using the algorithm developed in this paper, for the difference between computed and exact ground state energies for trial state  $\psi_{T1}$  (circles) and trial state  $\psi_{T2}$  (squares) using different values of the time step  $\tau$ . The  $\tau \rightarrow 0$  extrapolated values are also shown. For trial state  $\psi_{T1}$  we used  $\lambda = 1$ , the number of walkers was chosen to be  $N_w = 300$ , the number of Monte Carlo steps per walker was  $2 \times 10^7$ , and the acceptance rate was between 97% and 99.5%. For trial state  $\psi_{T2}$  we used  $\alpha = 0.001$ , the number of walkers was  $N_w = 100$ , the total number of Monte Carlo steps per walker was  $10^6$ , and the acceptance rate was the same as for  $\psi_{T1}$ . Since the parameter

$\alpha$  in  $\psi_{T2}$  was chosen so that  $\alpha \ll 1$ , the trial state and the corresponding Green's function were nearly exact and we were able to reach reasonable statistical accuracy with a relatively small number of Monte Carlo steps. As expected we find that when trial state  $\psi_{T1}$  is used the extrapolated energy agrees within statistical accuracy with the exact result, but when we use trial state  $\psi_{T2}$ , for which the phase is not exact, we obtain a variational upper bound for the exact ground state energy.

In Fig. 4 the density profiles for the exact ground state  $\psi_{gs} = \psi_{T1}(\lambda = 0)$  (Exact), the trial state  $\psi_{T1}(\lambda = 1)$  (VMC), the density obtained in FP DMC with trial state  $\psi_{T1}(\lambda = 1)$  at time step  $\tau = 0.001$  (FP mixed estimator), and the extrapolated density defined as ratio of the square of FP density to the variational density corresponding to  $\psi_{T1}(\lambda = 1)$ , are shown. Note that since the density in our DMC calculation is determined as a mixed estimate (see Eq. 15), and the density operator does not commute with the Hamiltonian between the DMC solution and the trial state, the corresponding density profile (FP mixed estimator) improves on the variational result but still differs from the exact density. The extrapolated estimator for the density constructed by combining both, the FP mixed estimator and the variational density makes it possible to improve on the FP density and is seen to be very close to the exact result.

*First Excited State ( $n = 1$ ):* As a further demonstration of the validity of our method we turn to the first excited state of the electron-monopole system. Again, we specify the  $L_{x^3}$  angular momentum quantum number and take  $m = \mathcal{S} + 1$  for which the exact excited state wave function is

$$\psi_{es} = \left( \frac{|z|}{z(1 + |z|^2)} \right)^{\mathcal{S}+1} |z| = |\psi_{es}| e^{i\varphi_{es}}. \quad (76)$$

We then introduce two new trial states

$$\psi_{T1} = \left( \frac{|z|}{z(1 + |z|^2)} \right)^{\mathcal{S}+1} \frac{|z|}{1 + \lambda|z|^2} = |\psi_{T1}| e^{i\varphi_{T1}} \quad (77)$$

and

$$\psi_{T2} = \left( \frac{|z|}{z(1 + |z|^2)} \right)^{\mathcal{S}+1} |z| \left( \frac{|z|}{z} \right)^\alpha = |\psi_{T2}| e^{i\varphi_{T2}} \quad (78)$$

with the property that for  $\lambda = 0$  and  $\alpha = 0$  they each reduce to the exact excited state,  $\psi_{es}$ . As before, for  $\lambda \neq 0$  and  $\alpha \neq 0$  the modulus of  $\psi_{T1}$  is approximate and the phase is exact ( $|\psi_{T1}| \neq |\psi_{es}|$ ,  $\varphi_{T1} = \varphi_{es}$ ) and the modulus of  $\psi_{T2}$  is exact and the phase is approximate ( $|\psi_{T2}| = |\psi_{es}|$ ,  $\varphi_{T2} \neq \varphi_{es}$ ).

Figure 5 shows the difference between FP DMC energies computed using trial states  $\psi_{T1}$  and  $\psi_{T2}$  and the exact excited state energy for different values of time step  $\tau$  as well as the extrapolated  $\tau = 0$  result. The parameters (number of walkers, number of Monte Carlo steps, etc.) used for these simulations were the same as those used for the ground state simulations except that we took  $\alpha = 0.0015$  in  $\psi_{T2}$ . Again, our simulations gave the expected results — when the phase of the trial state is exact we obtain the exact energy (circles),  $E_1 = (3/2 + 1/\mathcal{S})\hbar\omega_c$ , and when the phase is approximate we obtain a variational upper bound on that energy (squares).

In Figure 6 the density profiles corresponding to the trial state  $\psi_{T1}(\lambda = 1)$  (VMC), the FP density using the same state at time step  $\tau = 0.001$  (FP mixed estimator), the extrapolated density, computed as above by taking the ratio of square of the FP density and the VMC density (Extrap. estimator), and the exact density (Exact). The results are qualitatively similar to those for the ground state – the FP estimator improves on the VMC result, and the extrapolated density is nearly equal to the exact excited state density.

The simulation results presented in this Section provide a simple test of both the FP DMC method and the method developed in this paper for dealing with quantum corrections due to curvature. The results clearly show that these methods can be used to study quantum systems on curved manifolds.

## VI. DISCUSSION AND CONCLUSIONS

In this paper we have introduced a stochastic method to solve the many-body Schrödinger equation on curved manifolds. This method is essentially a generalized Diffusion Monte Carlo (DMC) technique allowing one to deal with the effects arising from the space curvature. We have shown that due to the curvature the diffusion matrix and drift vector, which appear in the Green's function used as a conditional probability in DMC simulations, acquire additional terms, the so-called quantum corrections. The explicit expressions for a general metric tensor are worked out in detail. Since the presence of the curvature leads to a number of other nontrivial modifications, we have presented a step by step algorithm which can be used to implement a code dealing with DMC simulations in curved space.

It is worth emphasizing that our method can be applied to a wide variety of inhomogeneous systems (e.g., inhomogeneous semiconductors with a position dependent effective mass), not just systems on curved manifolds. The reason for this, as discussed in Section III, is that the quantum corrections to the Green's function can be interpreted as being due to those terms which appear in the generalized diffusion equation describing the system once each of the derivatives in that equation have been commuted all the way to the left of each term. This definition of quantum corrections is quite general and can be applied to *any* differential equation which is second order in space and first order in time, regardless of the number of dimensions or any spatial inhomogeneity in the system.

To illustrate the general methodology we have concentrated on the problem of interacting fermions in external electromagnetic potentials. In this case a variational upper bound to the exact ground state energy can be found by applying the Fixed-Phase approximation, where the fermionic problem is treated as a bosonic one by fixing the phase of the many-body wave function (which is complex-valued in general) by some trial phase. As an example, we have considered the problem of a single electron confined to the surface of a two-sphere, which has a magnetic monopole at its center. The electron thus moves in a space with curvature in the presence of a magnetic field which breaks time-reversal symmetry. This simple problem can be solved in closed form and, therefore, we have used it as a playground for testing our technique. In the paper we have presented two calculations, where the ground and first excited state energies are computed using the exact phases, but approximate modulus for the corresponding guiding functions. We have shown that the exact energies are reproduced within statistical accuracy thus proving that the approach for dealing with the quantum corrections is valid.

As emphasized in the Introduction, the method presented in this paper for performing DMC simulations on curved manifolds can be used to study many interesting physical systems. An important example is the quantum Hall effect, a phenomenon which occurs when a two-dimensional electron system is placed in a strong magnetic field. As first pointed out by Haldane [22], the electron-monopole system described in Section V provides a convenient geometry for performing finite size numerical studies of quantum Hall systems when many interacting electrons are placed on the sphere. This is in part because the spherical geometry has no boundary so that finite size effects are suppressed. In addition, the spherical geometry is conceptually simpler than the (flat metric) torus geometry, which also has no boundary, because the topological order exhibited by quantum Hall states leads to certain nontrivial degeneracies on the torus [24].

Recently we have used the method developed in this paper to study some of the exotic excitations which occur in quantum Hall systems, specifically the fractionally charged quasiparticle excitations of the fractional quantum Hall effect [25], and the charged spin texture excitations (skyrmions) of the integer quantum Hall effect [26]. Previous numerical studies of these excitations have been based on either VMC or exact diagonalization calculations which, for the most part, have assumed that the wave functions describing the excitations are confined to the lowest ( $n = 0$ ) Landau level. In fact, this is a rather poor approximation for real experimental systems which can exhibit significant mixing of higher Landau levels due to the electron-electron interaction. Because the FP DMC method allows one to go beyond the lowest Landau level approximation it can be used to study the effect of Landau level mixing on quantum Hall states [7] and, by employing the method described in this paper, we were able to perform such studies using Haldane's spherical geometry. These simulations have provided useful quantitative results for various properties of quantum Hall excitations for realistic experimental parameters [25,26]. Along with the more rigorous test case of the electron-monopole system described in this paper, these calculations of Landau level mixing effects in quantum Hall systems using the Haldane sphere have shown that the method we have developed for performing FP DMC calculations on curved manifolds works well and can be used to study many other interesting physical systems.

## ACKNOWLEDGMENTS

We acknowledge stimulating discussions with David Ceperley. VM is supported by NSF grant number DMR-9725080. NEB is supported by US DOE grant number DE-FG02-97ER45639. Work at Los Alamos is sponsored by the US DOE under contract W-7405-ENG-36.

## REFERENCES

- [1] D.C. Mattis, *The Many-Body Problem* (World Scientific, Singapore, 1993).
- [2] For an introduction see, e.g., J.W. Negele and H. Orland, *Quantum Many-Particle Systems* (Addison Wesley, Redwood City, 1988), Ch. 8.
- [3] P.W. Anderson, *Basic Notions of Condensed Matter Physics* (Addison Wesley, Reading, 1984).
- [4] D.M. Ceperley, in *Recent Progress in Many-Body Theories*, edited by E. Schachinger, H. Mitter, and M. Sormann (Plenum, 1995).
- [5] L. Parker, Phys. Rev. D **22**, 1922 (1980).
- [6] C. Yannouleas, E. N. Bogachek, and U. Landman, Phys. Rev. B **53**, 10225 (1996).
- [7] G. Ortiz, D.M. Ceperley, and R.M. Martin, Phys. Rev. Lett. **71**, 2777 (1993).
- [8] L. Landau, Z. Phys. **64**, 629 (1930).
- [9] C. Kreft and R. Seiler, J. Math. Phys. **37**, 5207 (1996).
- [10] *Perspectives in Quantum Hall Effects*, edited by S. Das Sarma and A. Pinczuk (Wiley, New York, 1997).
- [11] F. Langouche, D. Roekaerts, and E. Tirapegui, Il Nuovo Cimento **53 B**, 135 (1979).
- [12] L.D. Landau and E.M. Lifshitz, *The Classical Theory of Fields* (Butterworth-Heinemann, Oxford, 1999), Ch. 10.
- [13] M. Hamermesh, *Group Theory* (Addison Wesley, Reading, 1962).
- [14] For a discussion of quantum corrections see, for example, B.S. DeWitt, Rev. Mod. Phys. **29**, 377 (1957); and D.W. McLaughlin and L.S. Schulman, J. Math. Phys. **12**, 2520 (1971).
- [15] A. M. Polyakov, *Gauge Fields and Strings* (Harwood, Chur, 1993), p.176.
- [16] R. P. Feynman and A. R. Hibbs, *Quantum Mechanics and Path Integrals* (Mc Graw-Hill, New York, 1965), Ch.4.
- [17] L. Onsager and S. Machlup, Phys. Rev. **91**, 1505 (1953).
- [18] For real symmetric Hamiltonians, this catastrophe is known as the “fermion-sign” problem. For a recent study, see M.H. Kalos and K.E. Schmidt, J. Stat. Phys. **89**, 425 (1997).
- [19] F. Wilczek, *Fractional Statistics and Anyon Superconductivity* (World Scientific, Singapore, 1990).
- [20] G. Ortiz and D.M. Ceperley, Phys. Rev. Lett. **75**, 4642 (1995).
- [21] P.J. Reynolds, D.M. Ceperley, B.J. Alder, and W.A. Lester, Jr., J. Chem. Phys. **77**, 5593 (1982).
- [22] F.D.M. Haldane, Phys. Rev. Lett. **51**, 605 (1983).
- [23] T.T. Wu and C.N. Yang, Nucl. Phys. B **107**, 365 (1976).
- [24] F.D.M. Haldane, Phys. Rev. Lett. **61**, 1029 (1988).
- [25] V. Melik-Alaverdian, N.E. Bonesteel, and G. Ortiz, Phys. Rev. Lett. **79**, 5286 (1997).
- [26] V. Melik-Alaverdian, N.E. Bonesteel, and G. Ortiz, Phys. Rev. B **60**, R8501 (1999).

# FIGURES

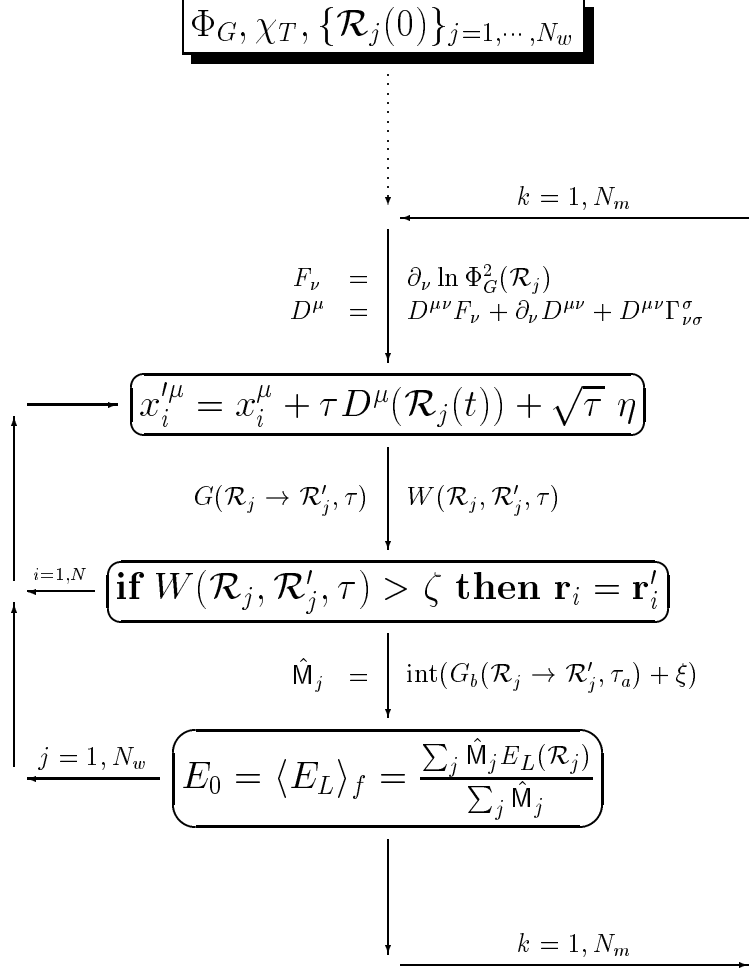


FIG. 1. A schematic of the Fixed-Phase method for curved manifolds with general metric  $g^{\mu\nu}$ . See the text for notation.

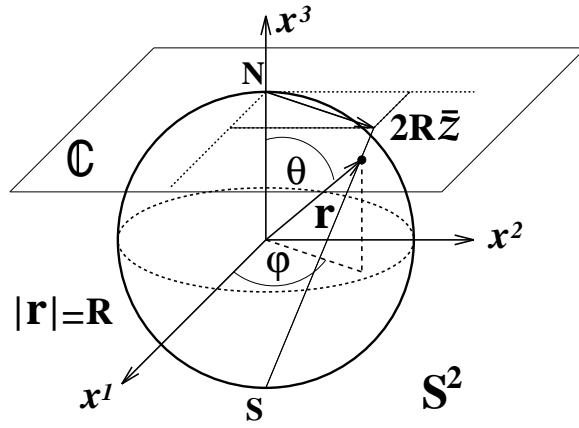


FIG. 2. Spherical and stereographic projection coordinates.  $R$  is the radius of the two-sphere  $S^2$ . Notice that points on the sphere are projected into the complex plane ( $z \in \mathbb{C}$ ) from the southern pole.



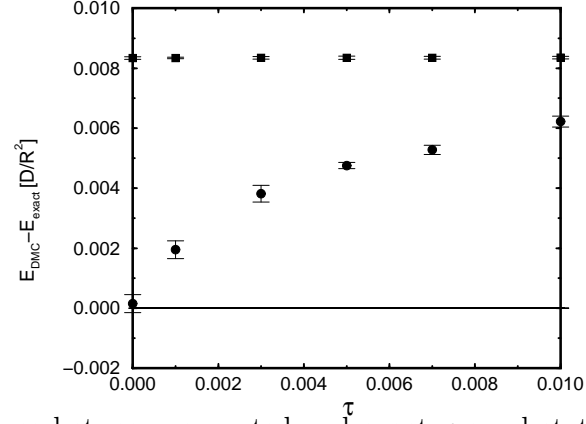


FIG. 3. The difference between computed and exact ground state energies for the trial state with the exact phase  $\psi_{T1}$  (circles) and the trial state with an approximate phase  $\psi_{T2}$  (squares) for various values of time step  $\tau$ . The  $\tau = 0$  extrapolated results are also displayed. Using a trial state with the exact phase in the FP DMC simulations allows one to solve the problem exactly, while using a trial state with an approximate phase allows one to obtain a variational upper bound for the exact solution.

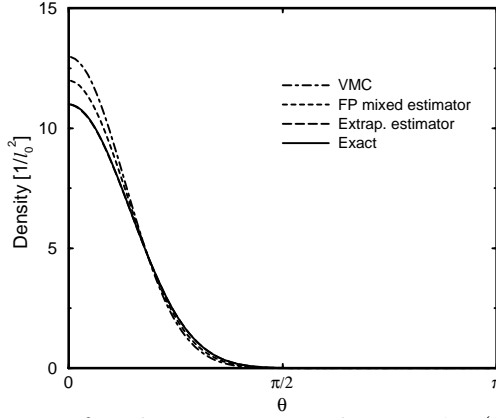


FIG. 4. Ground state density for the exact ground state  $\psi_{T1}(\lambda = 0)$  (Exact), the trial state  $\psi_{T1}(\lambda = 1)$  (VMC), the density obtained in FP diffusion Monte Carlo with trial state  $\psi_{T1}(\lambda = 1)$  at time step  $\tau = 0.001$  (FP mixed estimator), and the extrapolated density defined as ratio of the square of FP density to the variational density. The diffusion Monte Carlo density (FP mixed estimator) improves on the variational result but still differs from the exact one. The extrapolated estimator for the density constructed by combining both, the FP mixed estimator and the variational density makes it possible to improve on FP density and is very close to the exact result. The density is normalized in such a way that its integral over the surface of the sphere is  $4\pi R^2$ . The magnetic length is  $l_0 = \sqrt{\hbar c / |e|B}$ .

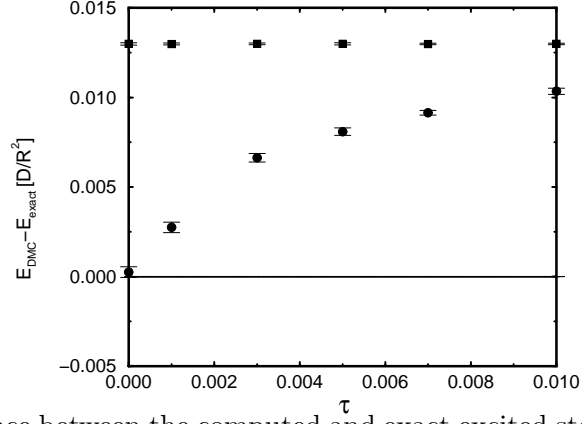


FIG. 5. The difference between the computed and exact excited state energies for the trial state with the exact phase  $\psi_{T1}$  (circles) and the trial state with an approximate phase  $\psi_{T2}$  (squares) for various values of time step. The extrapolated results to time step  $\tau = 0$  are also displayed. For the trial state with the exact phase one finds the exact solution and for the trial state with an approximate phase one finds a variational upper bound for the exact solution.

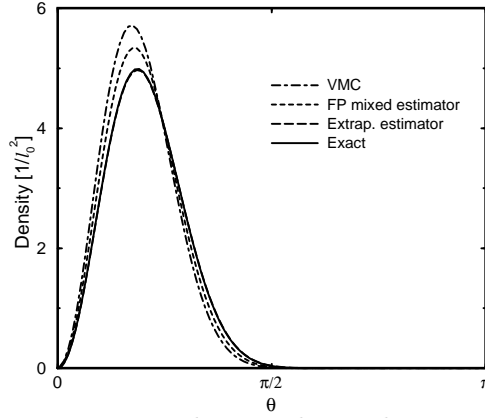


FIG. 6. Excited state density corresponding to the trial state  $\psi_{T1}(\lambda = 1)$  (VMC), FP density with the same state at time step  $\tau = 0.001$  (FP mixed estimator), the extrapolated density, which is computed by taking the ratio of square of the FP density and the VMC density (Extrap. estimator), and the exact density (Exact). The FP estimator improves on the VMC result, but still differs from the exact density. The extrapolated density allows one to improve on the FP diffusion Monte Carlo result and is very close to the exact. The density is normalized in such a way that its integral over the surface of the sphere is  $4\pi R^2$ .